

Supplementary Information

High-Dimension Ionic Memory in Oscillating Ion Current Signals

Anthony Dougman Cho,¹ Agata Wawrzekiewicz-Jałowicka,² Claudia E.P. Dewi,³ Shiwei Tang,¹ Ethan Cao,¹ Craig Martens,³ Tilman E. Schäffer,⁴ Javier Cervera,⁵ Patricio Ramirez,⁶ Salvador Mafe,^{5,7} Zuzanna S. Siwy^{1,*}

¹ Department of Physics and Astronomy, University of California, Irvine, USA

² Department of Physical Chemistry and Technology of Polymers, Silesian University of Technology, Gliwice, Poland

³ Department of Chemistry, University of California, Irvine, USA

⁴ Institute of Applied Physics, University of Tübingen, Germany

⁵ Dept. de Física de la Terra i Termodinàmica, Universitat de València, E-46100 Burjassot, Spain

⁶ Dept. de Física Aplicada, Universitat Politècnica de València, E-46022 València, Spain

⁷ Allen Discovery Center at Tufts University, Medford, MA, 02155-4243, USA

Table S1. Opening diameter of six nanopores that were used to collect data presented in this manuscript

Pore number	Base diameter (nm)	Tip diameter (nm)
Pore 1	1005	3
Pore 2	815	3
Pore 3	865	2
Pore 4 (SI only)	750	3
Pore 5	395	6
Pore 6 (SI only)	410	7

* Corresponding Author: zsiwy@uci.edu, Tel. 714-712-0027

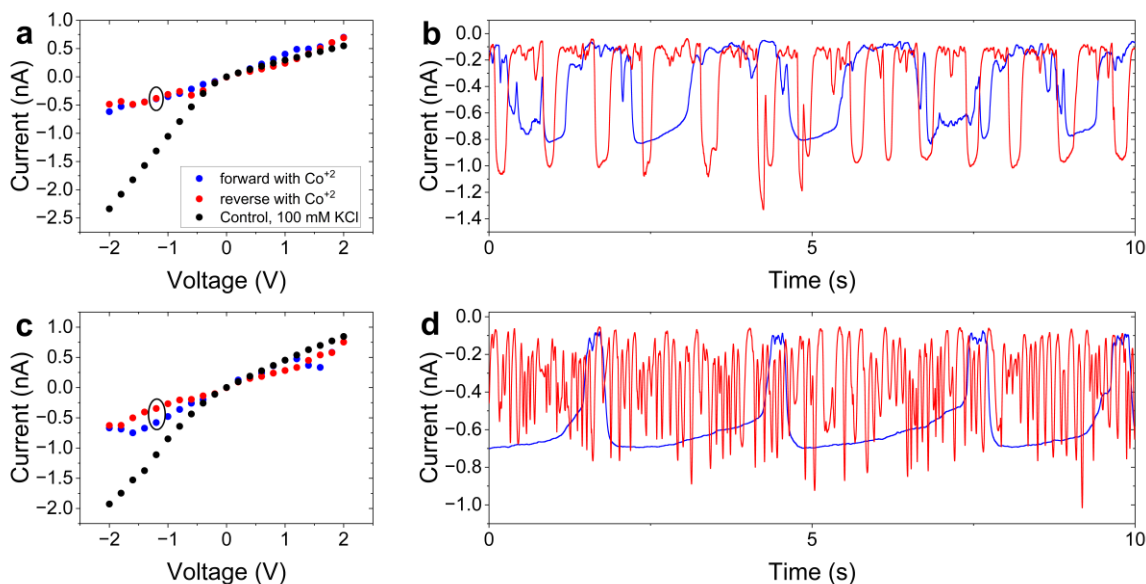


Figure S1. Current-voltage curves and fluctuations of ion current in time in forward and reverse voltage scans. (a,c) I-V curves and (b, d) recordings of ion current in time at -1.2 V of two independently prepared 3 nm in diameter pores (pores 4 (a,b) and 2 (c,d), Table S1). Pore 2 was also shown in Figures 1c and 1d in the main text. The I-V curves (a, c) were obtained by averaging as-recorded ion current time series in time. Note that pore 4 (panel a) and pore 2 (panel c) were held at each voltage for 15 s and 30 s, respectively. I-V curves shown as black circles correspond to recordings in 100 mM KCl and 2 mM PBS, while the data in blue and red show forward and reverse voltages scans, respectively in the additional presence of (a) 0.1 mM CoCl_2 , and (c) 0.05 mM CoCl_2 . The forward (reverse) voltage scans correspond to voltage scans from -2 V to +2 V (+2 V to -2 V). Ion current recordings shown in (b, d) were performed in -1.2 V with 100 mM KCl, 2 mM PBS, 0.1 mM CoCl_2 (b), and 100 mM KCl, 2 mM PBS, and 0.05 mM CoCl_2 (d). Red and blue recordings in (b,d) indicate the direction of the voltage scan when -1.2 V was reached. The data were filtered with a 10 Hz low pass filter.

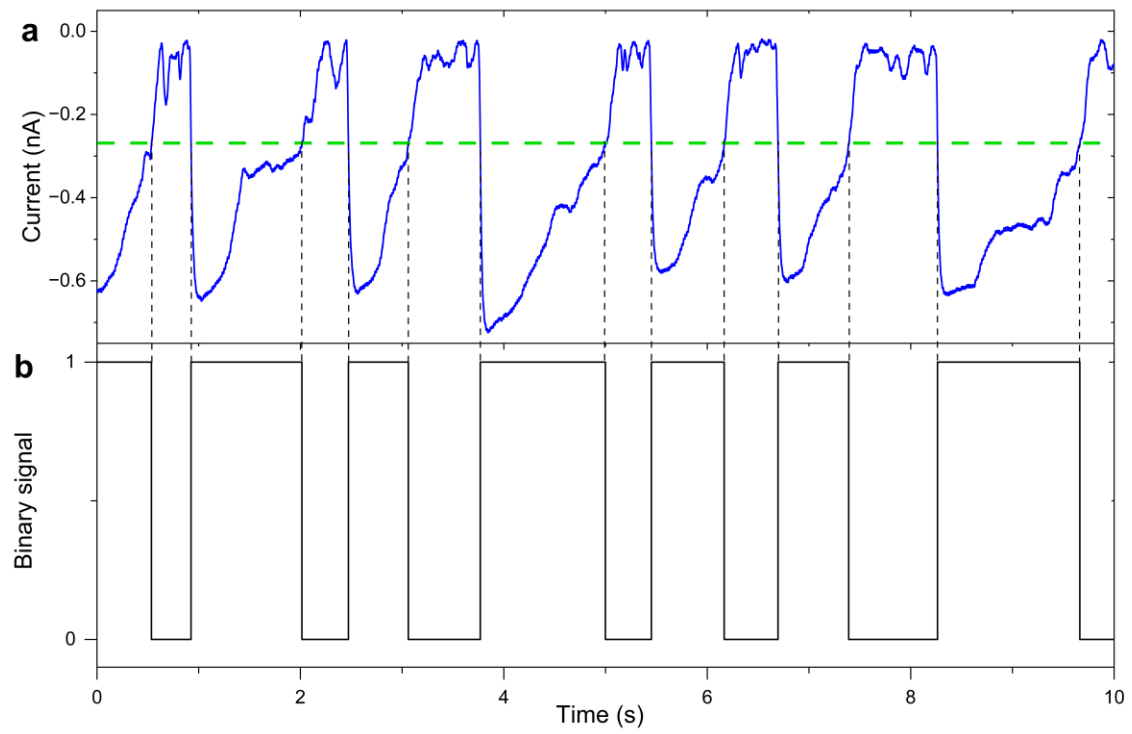


Figure S2. Binary ion current time series. (a) Example of raw ion current recordings and (b) corresponding binary signal. The green line in (a) represents the trigger value, $I_{trigger}$, that determines the transition between high (open) and low (closed) conductance states. In this time series, whenever the raw signal magnitude is larger than -0.27 nA, the binary current equals 1, and all other values are set as 0.

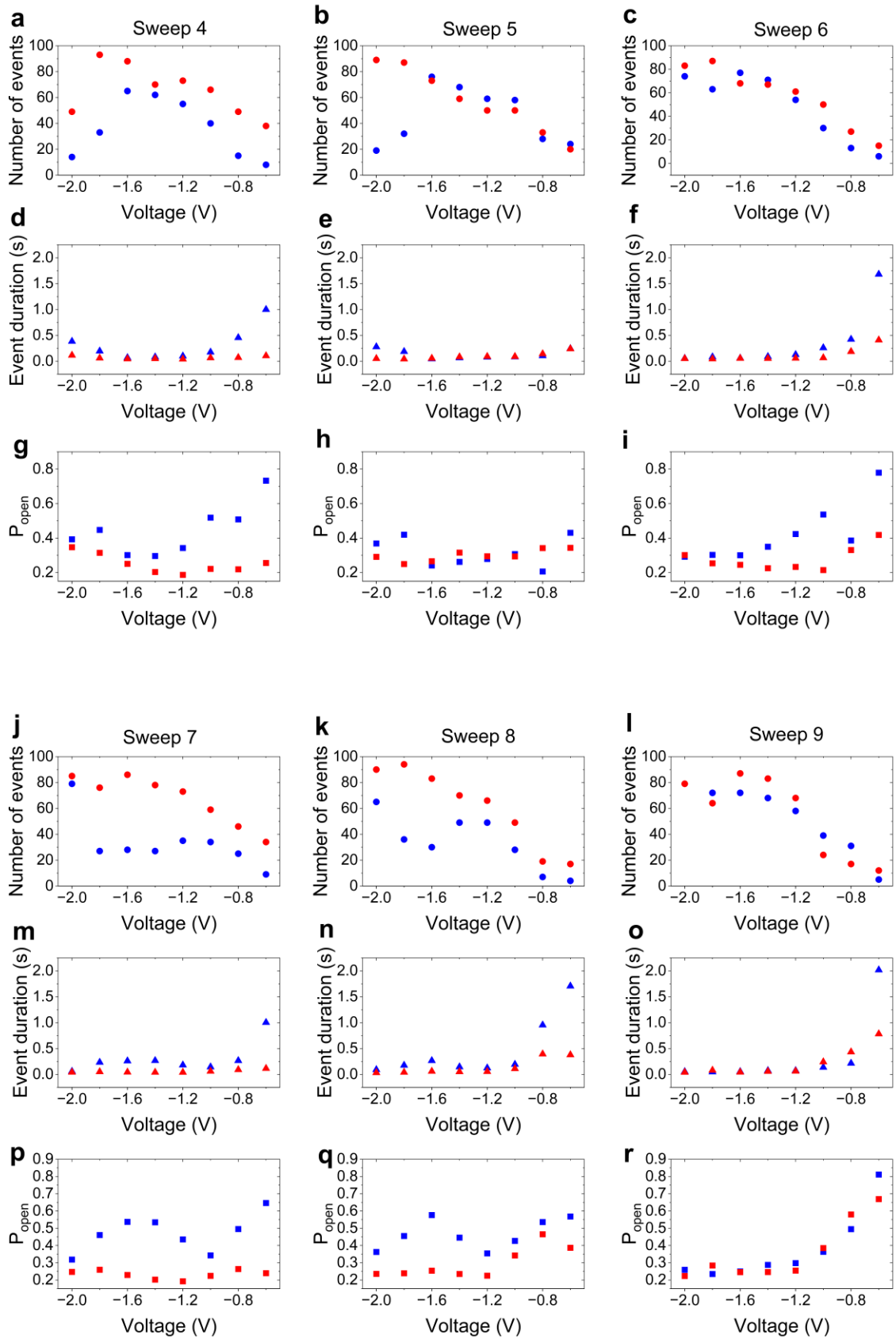


Figure S3. Analysis of 15 s long ion current time series recorded through a 3 nm in diameter pore in 100 mM KCl, 2 mM PBS, and 0.1 mM CoCl₂ as a function of voltage. *The same pore (pore 1) was shown in Figures 1a and 1b. Analysis of the first three sweeps is shown in Figure 2 in the main text. Points in red (blue) correspond to recordings in the reverse (forward) voltage sweeps. (a-c, j-l) Number of events of pore opening recorded in a 14 s interval at each voltage; the first second of the recording was not analyzed. (d-f, m-o) Average duration of open states. (g-i, p-r) Probability of pore in open state (P_{open}).*

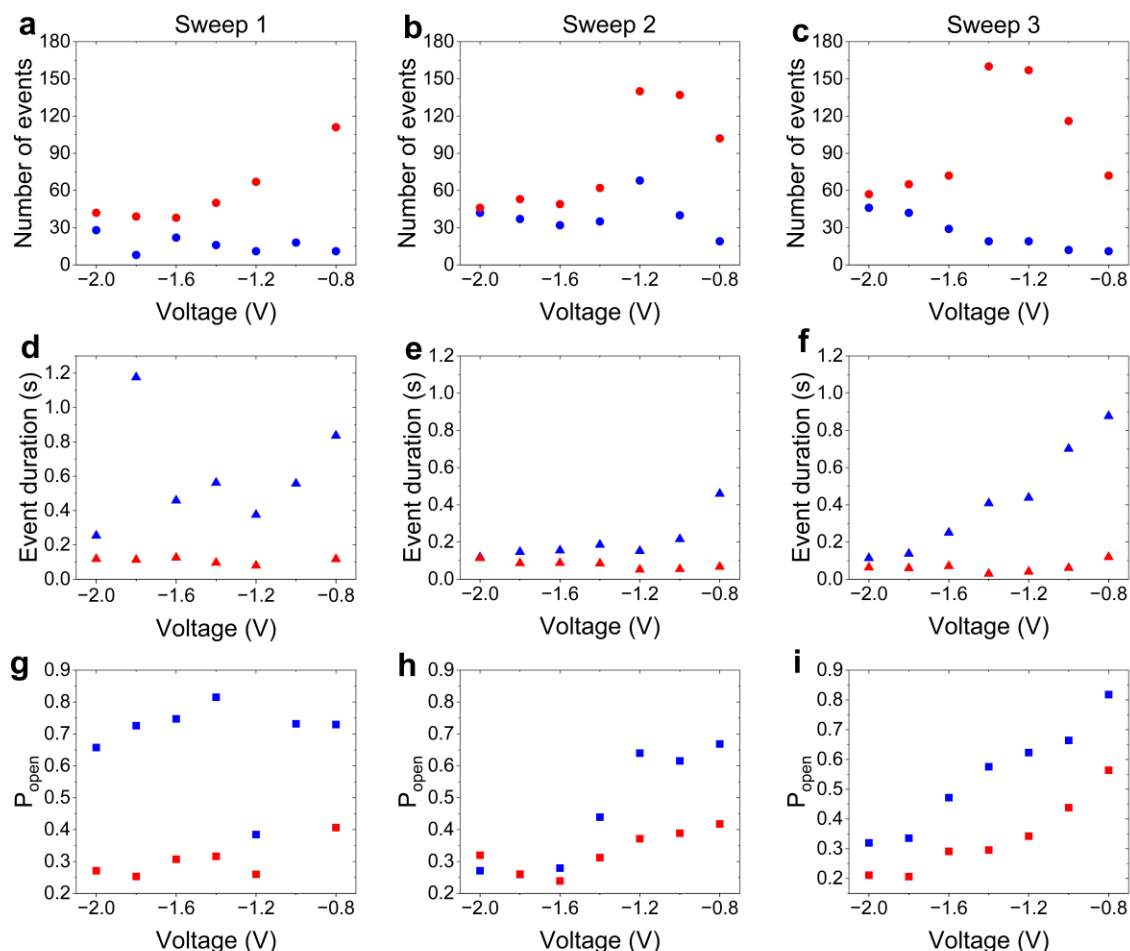


Figure S4. Analysis of 15 s-long ion current time series recorded through a 3 nm in diameter pore in 100 mM KCl, 2 mM PBS, and 0.05 mM CoCl_2 as a function of voltage. The same pore (pore 2) was analyzed in Figures 1c and 1d. Points in red (blue) correspond to recordings in the reverse (forward) voltage sweeps. The pore was subjected to three subsequent sweeps that are analyzed (columns). (a-c) Number of events of pore opening recorded in a 14 s interval at each voltage; the first second of the recording was not analyzed. (d-f) Average duration of open states. (g-i) Probability of pore in open state (P_{open}). At low negative voltages (> -0.8 V), there were no events detected within the time sampled. The voltage threshold is higher than for the pore shown in Figures 1a and 1b, likely due to the lower CoCl_2 concentration used.

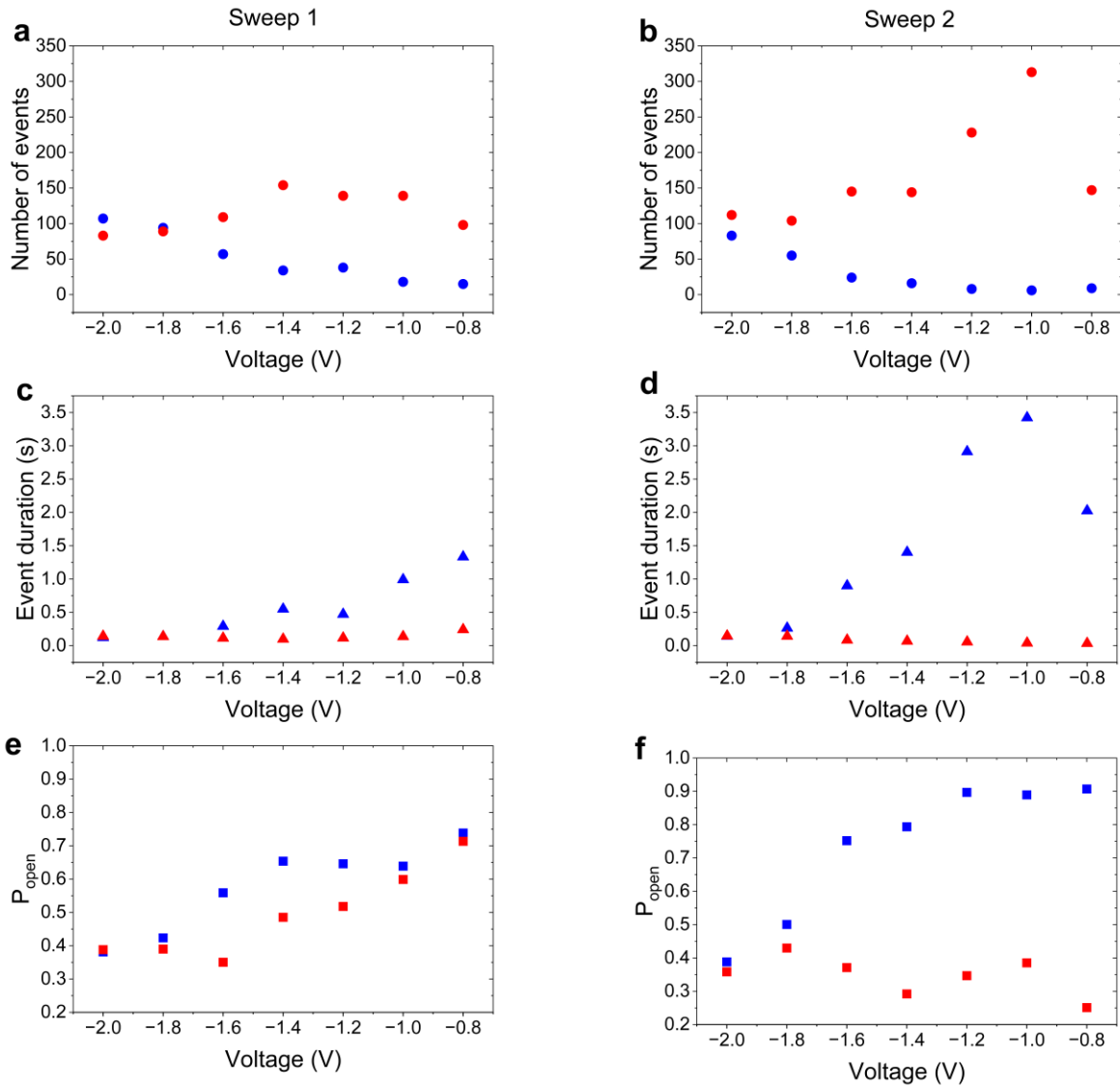


Figure S5. Analysis of 30 s long ion current time series recorded through a 3 nm in diameter pore in 100 mM KCl, 2 mM PBS and 0.05 mM CoCl_2 as a function of voltage. The same pore (pore 2) was shown in Figures 1c and 1d and analyzed in Figure S4. Points in red (blue) correspond to recordings in the reverse (forward) voltage sweeps. Two subsequent sweeps were recorded and analyzed (columns). (a-b) Number of events of pore opening recorded in a 30 s interval at each voltage. (c-d) Average duration of open states. (e-f) Probability of pore in open state (P_{open}). At low negative voltages (> -0.8 V), there were no events detected within the time sampled. The voltage threshold is higher than for the pore shown in Figures 1a and 1b, likely due to the lower CoCl_2 concentration used.

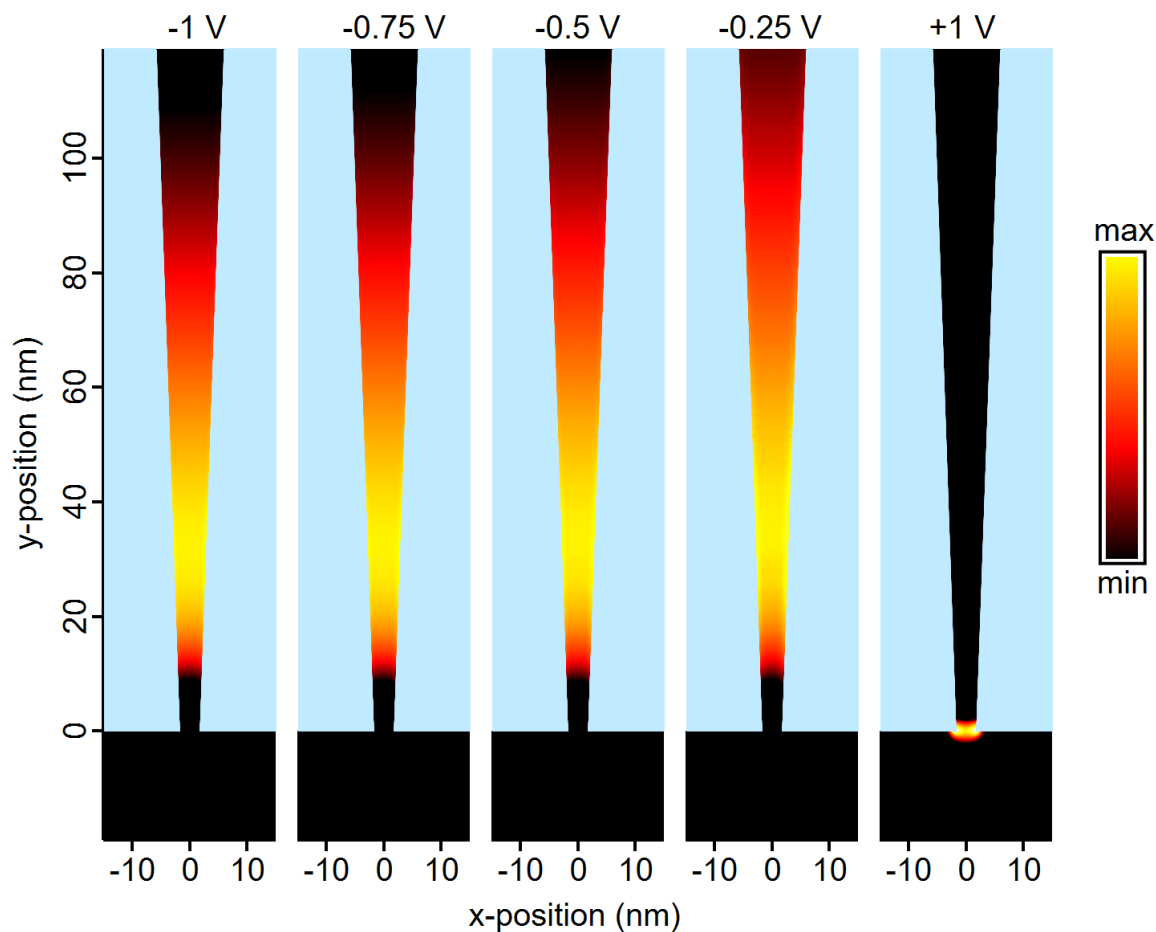


Figure S6. Results of finite elements modeling performed for a conically shaped nanopore with a tip diameter of 4 nm, length 3 μm , opening half-angle of 2° , and surface charge density of -0.05 C/m^2 . Product of the concentrations of a divalent cation and a divalent anion inside the pore volume. The reservoirs contained 0.1 M KCl, 0.1 mM CoCl_2 , and 2 mM K_2HPO_4 . The color scale for each voltage was set to represent 60 – 100% of the respective peak above the bulk value (0.2 mM^2): (min / mM^2 , max / mM^2) = (5.5, 9.0), (3.9, 6.3), (2.3, 3.7), (1.2, 1.8) and (0.69, 1.0) for -1.0 V, -0.75 V, -0.5 V, -0.25 V, and +1.0 V, respectively.

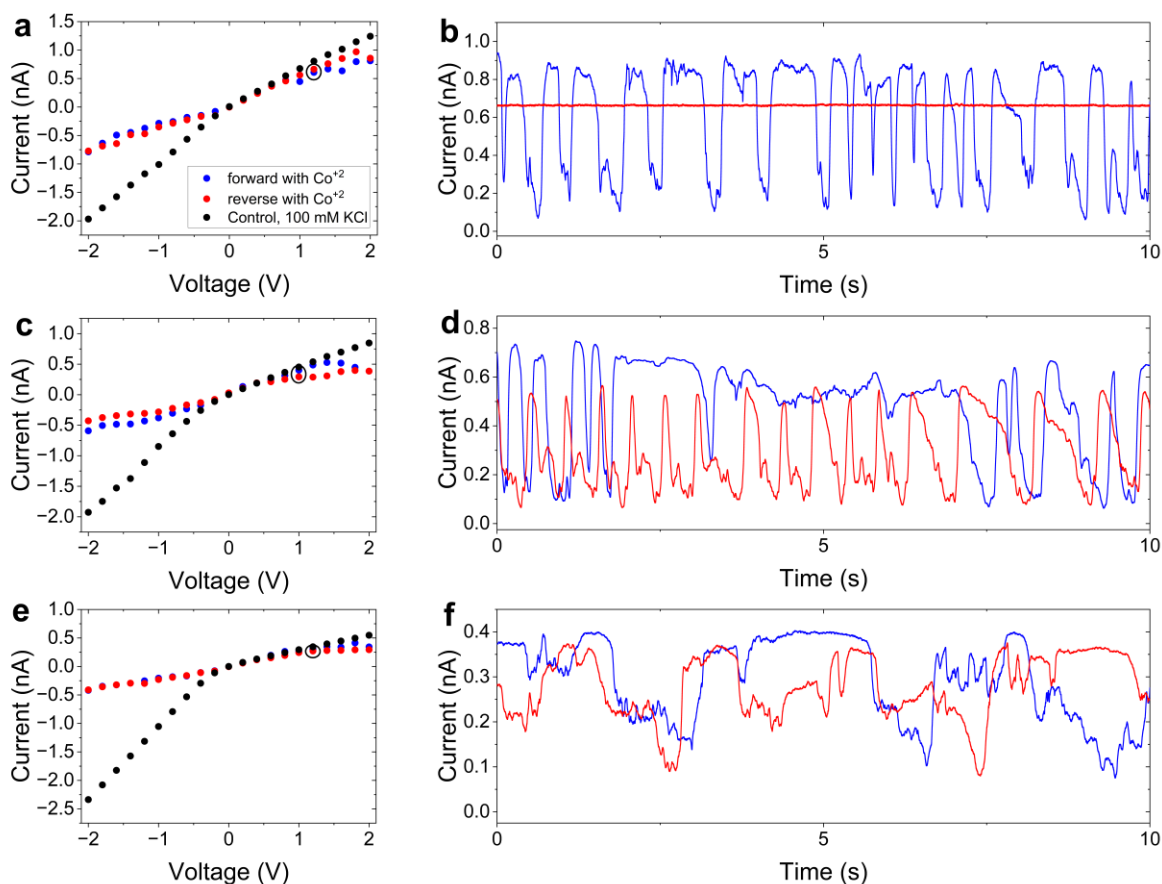


Figure S7. Current-voltage curves and fluctuations of ion current in time in forward and reverse voltage scans for positive voltages. (a, c, e) I-V curves and (b, d, f) recordings of ion current in time at +1.2 V of three independently prepared 2 and 3 nm in diameter pores (pores 1, 2 and 4 respectively). The I-V curves (a, c, e) were obtained by averaging as-recorded ion current time series in time. All pores were held at each voltage for 15 s. I-V curves shown as black circles correspond to recordings in a 100 mM KCl and 2 mM PBS for the three pores, while the data in blue and red show forward and reverse voltages scans, respectively, in the additional presence of 0.1 mM CoCl_2 (a, e) and 0.05 mM CoCl_2 (c). The forward (reverse) voltage scans correspond to voltage scans from -2 V to +2 V (+2 V to -2 V). Ion current recordings shown were performed in +1.2 V with 100 mM KCl, 2 mM PBS, and 0.1 mM CoCl_2 (b, f), and in 100 mM KCl, 2 mM PBS, and 0.05 mM CoCl_2 (d). Red and blue recordings indicate the direction of the voltage scan when +1.2 V was reached. The data was filtered with a 10 Hz low pass filter.

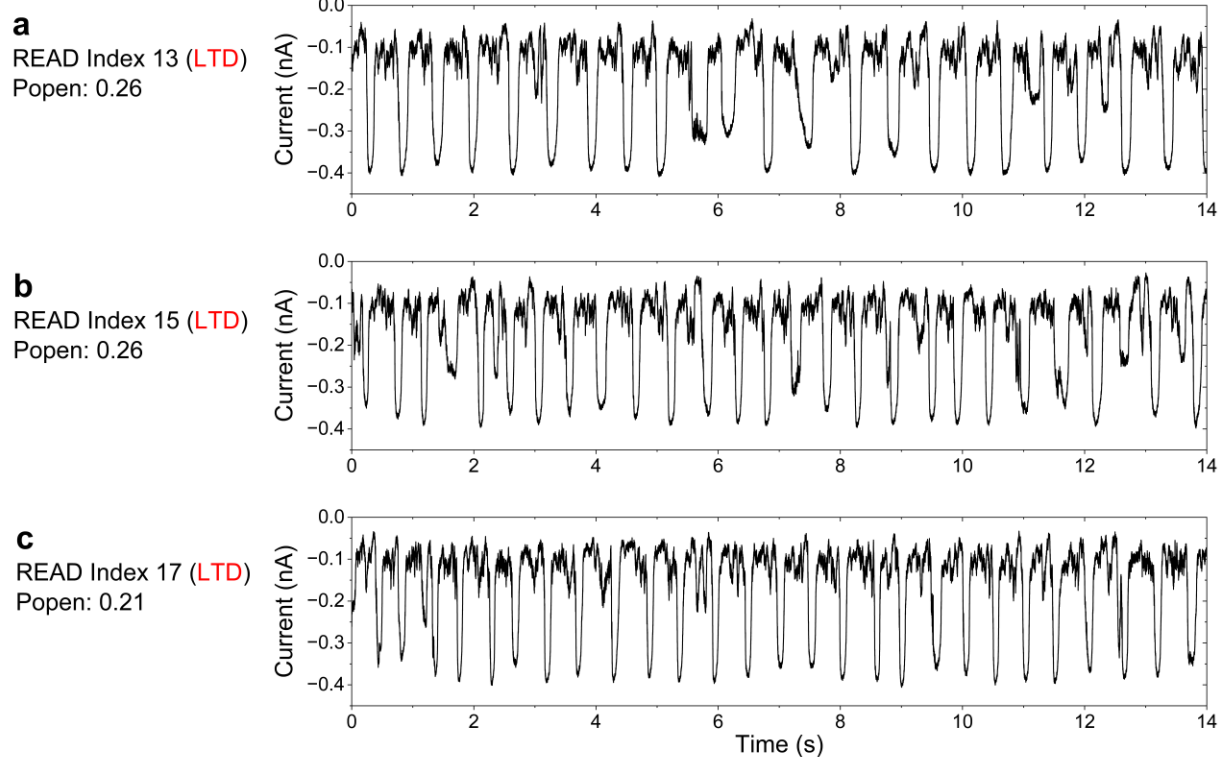


Figure S8. Example time series for a 2 nm in diameter conically shaped nanopore (pore 3) subjected to subsequent series of 15 s long LTD voltage pulses, applied after pulses shown in Figures 3c-3d in the main manuscript. Recordings were performed in 100 mM KCl, 2 mM PBS, and 0.1 mM CoCl_2 . (a-c) Recordings at non-consecutive READ voltages of index numbers 13, 15, and 17 (Figure 3a in the main text) are shown to indicate the system is gradually developing faster kinetics of current switching.

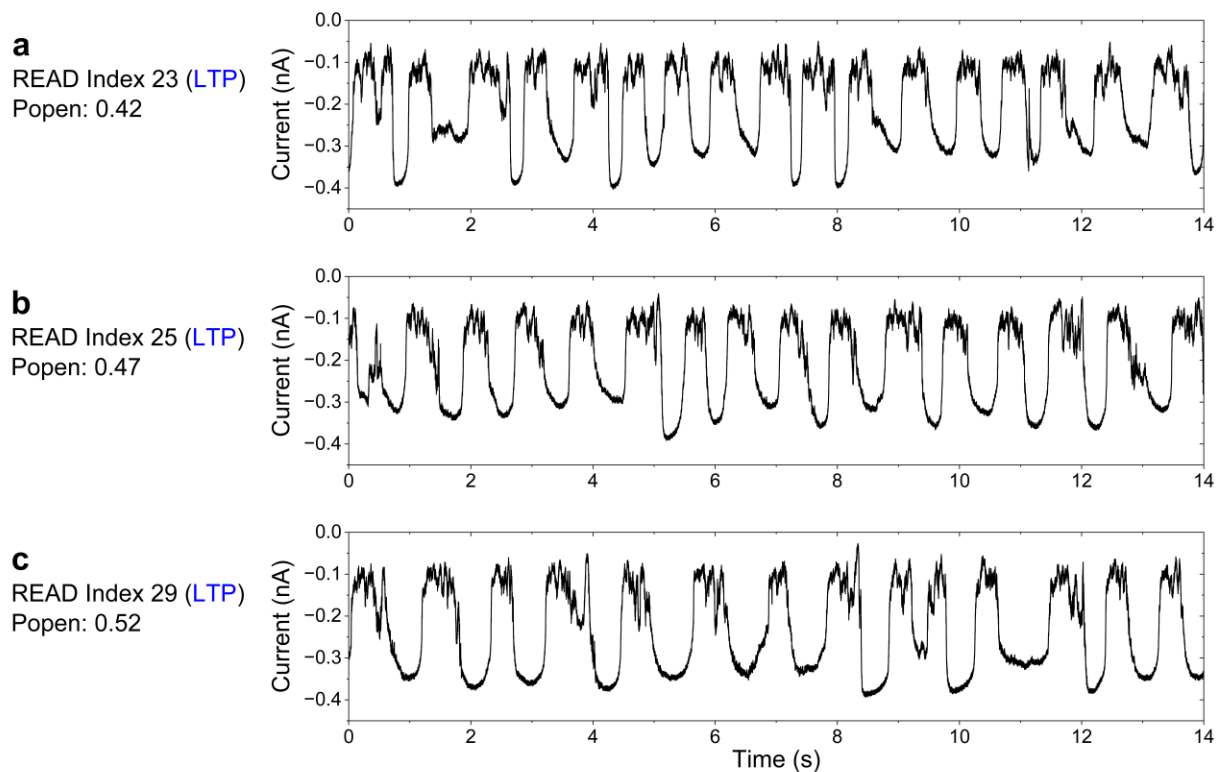


Figure S9. Example time series for a 2 nm in diameter conically shaped nanopore (pore 3) subjected to subsequent series of LTP voltage pulses, applied after pulses shown in Figures 3f-3g. Recordings were performed in 100 mM KCl, 2 mM PBS, and 0.1 mM CoCl₂. (a-c) Recordings at non-consecutive READ voltages of index number 23, 25, and 29 (Figure 3a in the main text) are shown to indicate the system gradually develops into an oscillatory behavior with slower kinetics.

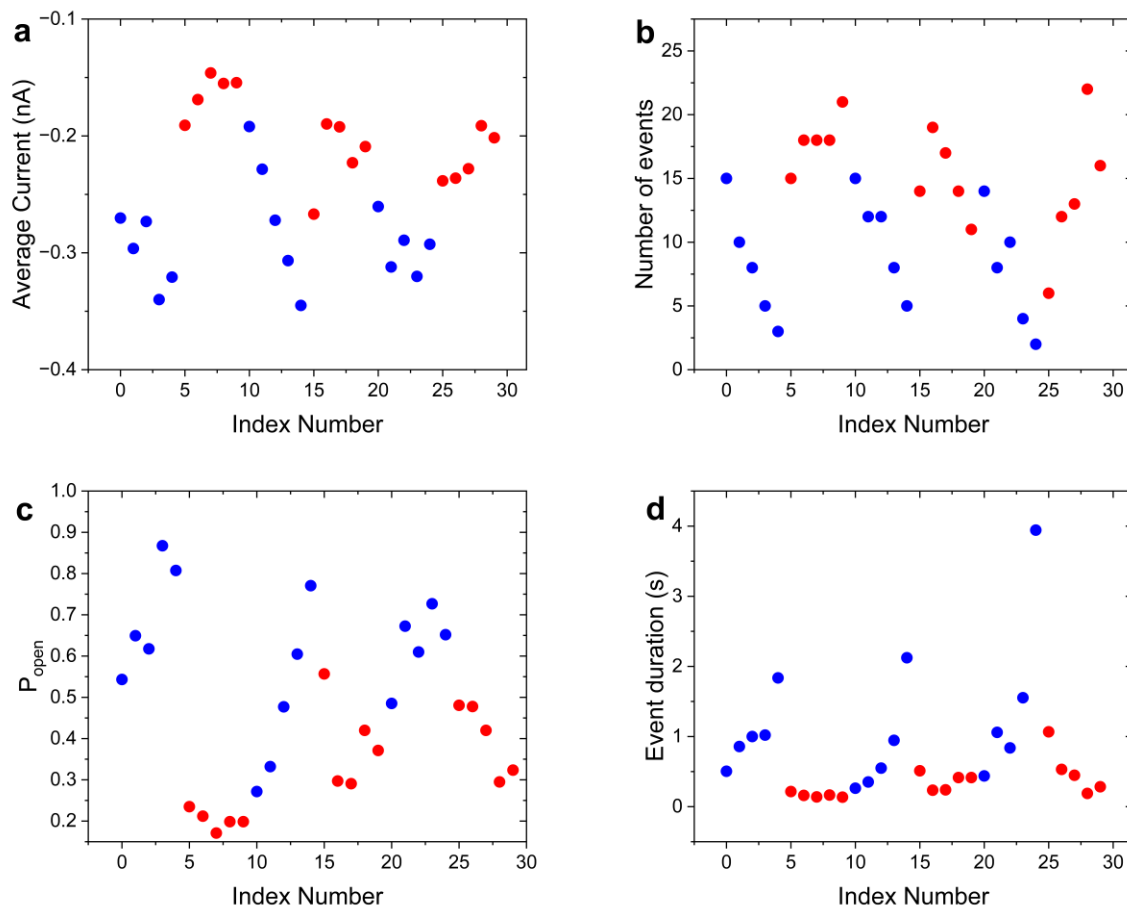


Figure S10. Analysis of pulse experiments performed with pore 4. Analogous analysis was performed in Figure 4 for pore 3. Ion current was recorded at READ voltage pulses of -1 V in 100 mM KCl, 2 mM PBS, and 0.1 mM CoCl_2 . LTP and LTD pulses were alternated after 5 subsequent pulses, according to a similar protocol as shown in Figure 3a. (a) Average current versus pulse index calculated from raw ion current recordings. (b-d) Analysis of READ time series event patterns. (b) Number of events, (c) P_{open} , and (d) event duration versus pulse index. Blue points represent READ time series subsequently after an LTP pulse, and red points represent READ time series subsequently after an LTD pulse.

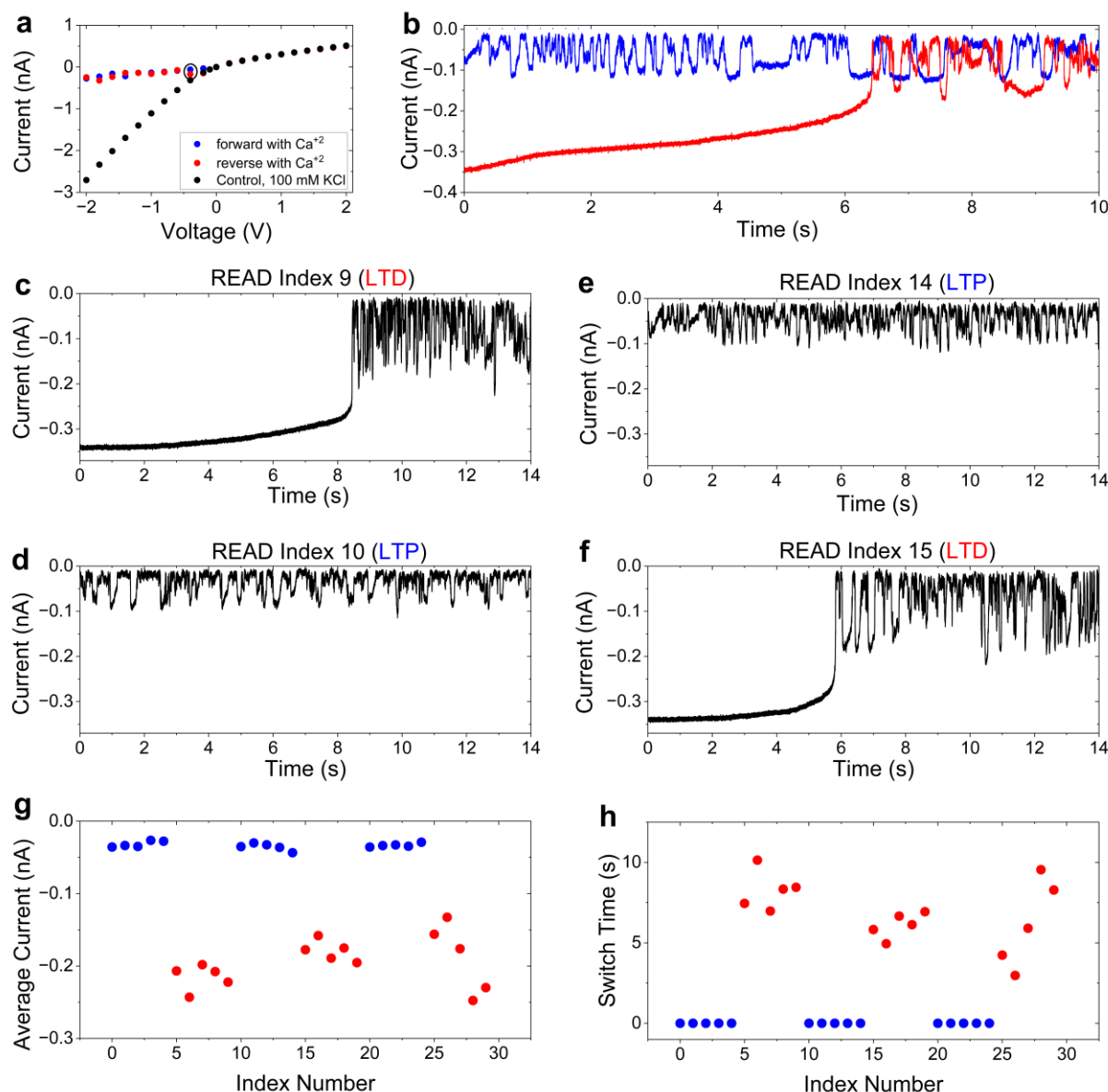


Figure S11. Calcium-induced ion current oscillations at low voltages. (a) I-V curves and (b) recordings of ion current in time at -0.4 V for a nanopore with an opening diameter of 7 nm (pore 6, Table S1). The I-V curves were obtained by averaging as-recorded ion current time series in time. I-V curves shown as black circles correspond to recordings in 100 mM KCl and 2 mM PBS, pH 8, while the data in blue and red show forward and reverse voltage scans, respectively in the presence of 100 mM KCl, 2 mM PBS, and 0.5 mM CaCl_2 . The forward (reverse) voltage scans correspond to voltage scans from -2 V to +2 V (+2 V to -2 V). (b) Ion current recordings at -0.4 V for both voltage scans in the presence of calcium salt. (c-f) Example time series for the same pore while subjecting the pore to 5 consecutive voltage pulses. All recordings were made at READ voltage -0.4 V. Series (c, f) were recorded after the pore had been subjected to +1.2 V (LTD pulse). Series (d, e) were conducted after the pore had been subjected to -1.2 V (LTP pulse). (g) Average current, and (h) Amount of time for the pore to fully close, versus pulse index.

In Figures S11 c,f, after LTD, +2 V, pulses are applied, in the first ~6 s, the pore remains in the high conductance state, followed by a slow decrease before fully entering the low conductance state and the onset of current instabilities. This is a qualitatively different type of memory than that presented in the rest of the manuscript, since the memory is observed in the amount of time for the current to begin oscillations and in average current (Figures S11g and S11h). In addition, the direction of memory is the opposite to what we show in Figures 1-5 in the main text. In this lower voltage regime (-0.4 V), currents in the reverse sweep are less dynamic, and application of LTP signals lowers the current. This memory is reminiscent of previously reported memristors based on precipitation and hysteresis in I-V curves.^{1,2} Existence of two types of ionic memory in conical nanopores with precipitation could be explained through non-equilibrium behavior of the transmembrane current. A previous study has reported an existence of a small window of conditions where there are two Hopf bifurcation points, necessary to realize an oscillating current.³ At lower voltages, we are sampling a different section of phase space, close to the bifurcation point, where the overall memory trend is inverted. Namely, at the voltage range when the oscillations are not yet fully developed, subsequent LTP and LTD signals push the system towards oscillating/fluctuating and fully open states, respectively, for the first few seconds after the pulse is applied. At higher voltages, on the other hand, LTP and LTD signals switch the system between two oscillating states that are characterized by different frequencies of oscillations, and this behavior occurs in the parameter space beyond the bifurcation points.

References

1. Laucirica, G., Toimil-Molares, M.E., Marmisollé, W.A. & Azzaroni, O. Unlocking Nanoprecipitation: A Pathway to high reversibility in nanofluidic memristors. *ACS Appl. Mater. Interfaces* **16**, 58818-58826 (2024).
2. Laucirica, G. et al. Insight into the transport of ions from salts of moderated solubility through nanochannels: negative incremental resistance assisted by geometry. *Nanoscale* **16**, 12599-12610 (2024).
3. Cordero, A., Torregrosa, J.R. & Bisquert, J. Bifurcation and oscillations in fluidic nanopores: A model neuron for liquid neuromorphic networks. *Phys. Rev. Res.* **7**, 013282 (2025).